

On quantum invariants and the graph isomorphism problem

P. W. Mills,¹ R. P. Rundle,^{1,2} J. H. Samson,¹ Simon J. Devitt,^{3,4}
Todd Tilma,^{5,1} V. M. Dwyer,^{1,2,*} and Mark J. Everitt^{1,†}

¹*Quantum Systems Engineering Research Group, Department of Physics,
Loughborough University, Loughborough, Leicestershire LE11 3TU, United Kingdom*

²*The Wolfson School, Loughborough University, Loughborough, Leicestershire LE11 3TU, United Kingdom*

³*Centre for Quantum Software & Information (QSI),*

*Faculty of Engineering & Information Technology,
University of Technology Sydney, Sydney, NSW, 2007, Australia.*

⁴*Turing inc., Berkeley, CA, 94701 USA*

⁵*Tokyo Institute of Technology, 2-12-1 Ookayama, Meguro-ku, Tokyo 152-8550, Japan*

(Dated: Saturday 14th December, 2024)

Three new graph invariants are introduced which may be measured from a quantum graph state and form examples of a framework under which other graph invariants can be constructed. Each invariant is based on distinguishing a different number of qubits. This is done by applying alternate measurements to the qubits to be distinguished. The performance of these invariants is evaluated and compared to classical invariants. We verify that the invariants can distinguish all non-isomorphic graphs with 9 or fewer nodes. The invariants have also been applied to ‘classically hard’ strongly regular graphs, successfully distinguishing all strongly regular graphs of up to 29 nodes. We find that a combination of the classical eigenspectra and our quantum invariant distinguishing one qubit can identify all the non-isomorphic graphs we consider in this work in $\mathcal{O}(N^3)$ gate operations and ensemble measurements for N node graphs. Our quantum invariant distinguishing two qubits is able to distinguish all graphs we have considered with $\mathcal{O}(N^4)$ gate operations and ensemble measurements. We discuss the experimental feasibility of our methods and possible extensions to important problems such as isomorphism weighted and fuzzy graphs.

I. INTRODUCTION

A graph is a set of nodes connected by edges, and two graphs are termed isomorphic if one may be obtained from the other by permuting the labels of their nodes [1]. The question of whether two graphs are isomorphic is the so-called graph isomorphism (GI) problem [2]; a computationally hard problem that is not just of academic interest, but is also central to a number of areas critical to industry. Some of the more obvious of these include the following: the IC industry requires designs to pass a key (layout versus schematic) verification check, which compares the transistor network delivered by the Logic Synthesizer to that extracted from the Place and Route engine [3]; in the field of image recognition, including registration problems in computer vision [4] and medical imaging (for example automated histology analysis [5]), graphs are used as effective structural descriptors due to their ability to represent relational information in which nodes are associated to image components and edges to the relationships between them; in the field of Cyber Security, the control flow graphs of a number of worms have been analysed as a detection technique [6]. Perhaps less obvious applications of GI involve [7]; financial fraud detection, banking risk management, legal precedents, fault detection and even zero-knowledge proofs [8]. The global worth of a number of these sectors has been estimated by

some industry experts to be up to £1Bn, making progress in solving the GI problem an important industrial as well as academic challenge [7].

Complexity arises here as, even restricted to simple undirected graphs without loops, the number of non-isomorphic graphs increases at least exponentially with the number of nodes [1]. The combination of a number of different methods has resulted in classical algorithms that are efficient for many graphs [9–11]. However, there still exist a large number of important graphs for which solutions do not currently exist [7]. As a result, new contributions to graph isomorphism, such as those that might be offered by quantum computing, would add real value; even if they only deal with these difficult cases.

While the problem is computationally hard, simple methods such as edge counting or spectral comparisons can resolve many cases efficiently. These comparisons rely on the fact that such properties (known as graph invariants [12]) are shared by all isomorphic graphs. The current best classical algorithm for the general case is due to Weisfeiler and Lehman [13–15] implemented in the Nauty algorithm [10] which is able to solve many cases of practical interest in polynomial time. However, a general solution with polynomial scaling does not exist, and recent unpublished work indicates that the problem is classically solvable in quasi-polynomial time, leaving GI between polynomial and exponential in its complexity [16, 17]. It is worth noting here that Nauty performs poorly for strongly regular graphs, graphs which the quantum algorithms developed here are able to distinguish (up to the 29 node graphs tested). This demon-

* v.m.dwyer@lboro.ac.uk

† m.j.everitt@physics.org

strates that our algorithms are fundamentally different from (at least two dimensional) Weisfeiler-Lehman methods [18, 19].

Two factors support the existence of an efficient algorithmic quantum solution for the graph isomorphism problem. The first is that the complexity of the GI problem is equivalent to that of integer factorization [20], a problem which can be solved in polynomial time on a quantum computer using the Shor algorithm [21]. The second reason follows from the existence of an adiabatic quantum-annealing method by Gaitan and Clark [22], which already solves the GI problem. As the algorithm is adiabatic, the method's complexity is unknown. However since adiabatic and algorithmic quantum computing are known to be equivalent [23], the adiabatic method guarantees the existence of a quantum solution. We also note here the work of Wang *et al.* [24, 25] applying quantum walks to the GI problem; these methods have successfully distinguished classes of strongly regular graphs with up to 64 nodes. Whilst we have been unable to analyse such large graphs due to the scaling of our classical simulations, we note that the scaling involved in obtaining the invariants presented below outperforms those of quantum walks when obtained on a quantum machine. Furthermore, since our approach is different from others it may be able to distinguish Cai-Fürer-Immerman graphs [18, 26]. The ability to distinguish such graphs would demonstrate our algorithms are distinct from all dimensions of the Weisfeiler-Lehman algorithm [19], as well as the quantum walks approach which has been shown to be equivalent to Weisfeiler-Lehman's [27].

Motivated by these factors we introduce a number of graph invariants which, to the authors knowledge, will only be efficiently determined on a quantum computer. These and the classical invariants are compared below for their efficiency in distinguishing graphs, as a function of graph node number. We have found that our invariants are better at distinguishing graphs than several classical methods in the sense that a higher proportion of graphs give a unique result. Indeed, in the worst case, the proportion of graphs which the quantum invariants cannot distinguish appears to tend to zero. In the particular case of strongly regular graphs, the quantum invariants are able to distinguish all graphs with less than 30 nodes. Furthermore, we find that two of our quantum measures allow all the non-isomorphic graphs that we have been able to consider in this work to be distinguished with a polynomial number of gate operations and ensemble measurements.

This work presents a family of quantum graph invariants that potentially could form part of a hybrid classical-quantum computing solution that, if realised on a suitable quantum information processor, might address the industrial needs identified above.

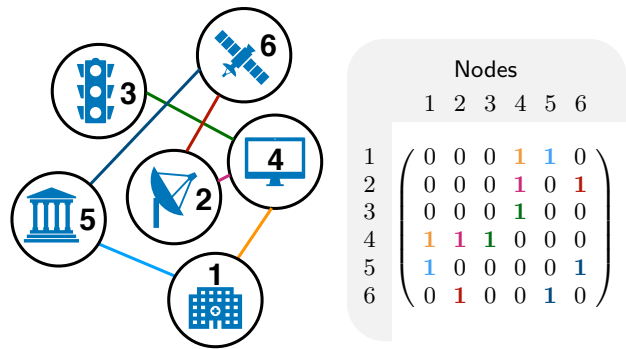


FIG. 1. Schematic showing an example network or graph and the associated adjacency matrix that represents it. The adjacency matrix is constructed by numbering each node and associating each row and column with a node. Ones are then entered into the positions corresponding to connected nodes and zeros otherwise. The set of adjacency matrices associated with isomorphic graphs are those that are formed from simultaneously permuting the matrices' rows and columns.

II. CONSTRUCTING GRAPH STATES

To study graphs in a quantum setting we first map them into quantum states known as graph states. To do so we follow the procedure described in the paper of Zhao *et al.* [28] which efficiently and uniquely encodes the graphs [29–32]. For convenience, we set out below the procedure given in [28] for making graph states. We then show it is possible to construct classes of measurements, derived from the Wigner function [33–35], which act as graph invariants.

To obtain a graph state from a graph or network, first the adjacency matrix must be found as shown in Fig. 1. A set of operators is then constructed from the adjacency matrix by replacing the elements of the adjacency matrix with Pauli matrices according to the following scheme: diagonal entries of the matrix are replaced by $\hat{\sigma}_x$; all other zeros are replaced by the identity operator, which we denote by $\hat{\sigma}_I$, and each '1' is replaced by a $\hat{\sigma}_z$. The tensor product is then taken between adjacent matrices within each row, resulting in a set of N operators for an N -qubit system. Note that each qubit corresponds to a node in the graph. For the adjacency matrix shown in Fig. 1, the corresponding set of operators is given by;

$$\left\{ \begin{array}{l} \hat{\sigma}_x \otimes \hat{\sigma}_I \otimes \hat{\sigma}_I \otimes \hat{\sigma}_z \otimes \hat{\sigma}_z \otimes \hat{\sigma}_I \\ \hat{\sigma}_I \otimes \hat{\sigma}_x \otimes \hat{\sigma}_I \otimes \hat{\sigma}_z \otimes \hat{\sigma}_I \otimes \hat{\sigma}_z \\ \hat{\sigma}_I \otimes \hat{\sigma}_I \otimes \hat{\sigma}_x \otimes \hat{\sigma}_z \otimes \hat{\sigma}_I \otimes \hat{\sigma}_I \\ \hat{\sigma}_z \otimes \hat{\sigma}_z \otimes \hat{\sigma}_z \otimes \hat{\sigma}_x \otimes \hat{\sigma}_I \otimes \hat{\sigma}_I \\ \hat{\sigma}_z \otimes \hat{\sigma}_I \otimes \hat{\sigma}_I \otimes \hat{\sigma}_I \otimes \hat{\sigma}_x \otimes \hat{\sigma}_z \\ \hat{\sigma}_I \otimes \hat{\sigma}_z \otimes \hat{\sigma}_I \otimes \hat{\sigma}_I \otimes \hat{\sigma}_z \otimes \hat{\sigma}_x \end{array} \right\} = \left\{ \begin{array}{l} \hat{G}_1 \\ \hat{G}_2 \\ \hat{G}_3 \\ \hat{G}_4 \\ \hat{G}_5 \\ \hat{G}_6 \end{array} \right\}. \quad (1)$$

These operators, \hat{G}_i , $i \in \{1, \dots, N\}$, are known as group generators, since their products form a finite abelian group of 2^N operators \hat{g}_k , $k \in \{1, \dots, 2^N\}$. Adding the group elements together and normalising gives the density matrix of the corresponding graph state. The density

matrix can also be expressed in a factorised form using only the generators as shown on the right [36]:

$$\hat{\rho} = \frac{1}{2^N} \sum_{k=1}^{2^N} \hat{g}_k = \frac{1}{2^N} \prod_{i=1}^N (\mathbb{1} + \hat{G}_i). \quad (2)$$

It is worth noting that graph states are a subset of stabilizer states [37]. They are pure states that are said to be fixed by the generators, i.e. $\hat{G}_i \hat{\rho} = \hat{\rho}$. It is the form of the states which makes using graph states so promising for producing effective graph invariants. This is because all the information about the graph is in the state and every group element is accessible either individually or simultaneously via measurements. Hence all the information is available and it is just a question of generating schemes for efficiently accessing the relevant information.

Zhao [28] also covers how to experimentally construct the states expressed in Eq. (2). First, each node is associated with a qubit prepared in the $+1$ eigenstate of $\hat{\sigma}_x$; $|+\rangle$. Controlled-Z gates are then applied between any two qubits whose corresponding nodes are connected in the graph. For a fully connected quantum computer this procedure requires $\mathcal{O}(N^2)$ operations. However, it has been shown by Zhao that it is theoretically possible to construct graph states with $\mathcal{O}(N)$ operations with the use of an oracle.

We note that it is also possible to implement the procedure on hardware with limited connectivity provided a path of connections can be found between any two qubits connected in the graph. Regarding the current IBM machines, a CZ gate is not provided as required in the algorithm to generate graph states. This problem is easily overcome by adding appropriate Hadamard gates to the CNOT gates. In cases where there is less connectivity and there is no direct CNOT gate between two qubits, it is possible to ‘skip’ a qubit with a sequence of CNOT gates, provided both of the qubits have a connection to a shared qubit. Although possible, the number of gates needed to ‘skip’ higher number of qubits grows quickly, resulting in higher decoherence in the algorithm. A similar sequence of gates is also possible with CZ gates with a similar outcome. Thus it is possible to implement our algorithm on various architectures, as long as a minimum connectivity is met.

III. METHODS

A. Underpinning theory

Having described how to encode a graph into a graph state, we now discuss how to measure its quantum graph invariants. An observable can only be a quantum graph invariant if its measurement results do not depend upon the order in which the qubits are labelled. Two ways of achieving such a measurement are to treat all qubits identically or to measure each qubit individually and then

discard ordering information by sorting the individual measurement results according to some arbitrary norm, for example by magnitude. The former case is order invariant for any given state since the measurement results contain no qubit index information and therefore the order in which the qubits are labelled must have no effect.

If we consider a general measurement on N qubits

$$\hat{M} = \bigotimes_{j=1}^N \hat{m}_j \quad (3)$$

then the former case corresponds to taking $\hat{m}_j = \hat{m}$ for all j giving,

$$\hat{M}_0 = \hat{m}^{\otimes N}. \quad (4)$$

While, as an example of the second case, we consider the situation in which the observable being measured on one arbitrary qubit \hat{m}_1 is different to the observable being measured on all other qubits \hat{m}_0 giving,

$$\hat{M}_1 = \bigotimes_{j=1}^N (\delta_{jq} \hat{m}_1 + (1 - \delta_{jq}) \hat{m}_0). \quad (5)$$

If this measurement is repeated for all $q \in \{1, \dots, N\}$, the expectation values lead to a quantum graph invariant once the values are sorted. Thus

$$\langle \hat{M} \rangle = \text{sort} \left(\langle \hat{M}_1^{(q=1)} \rangle, \langle \hat{M}_1^{(q=2)} \rangle, \dots, \langle \hat{M}_1^{(q=N)} \rangle \right) \quad (6)$$

In either case the expectation values of these operators may be calculated in a similar manner given below.

Expanding Eq. (2) the graph state may be written in terms of its generators as

$$\begin{aligned} \hat{\rho} &= \frac{1}{2^N} \prod_{i=1}^N (\mathbb{1} + \hat{G}_i) = \sum_{\underline{a}} \hat{G}_1^{a_1} \hat{G}_2^{a_2} \dots \hat{G}_N^{a_N} \\ &= \sum_{\underline{a}} \left(G_{1(1)}^{a_1} G_{2(1)}^{a_2} \dots G_{N(1)}^{a_N} \otimes \dots \otimes G_{1(N)}^{a_1} G_{2(N)}^{a_2} \dots G_{N(N)}^{a_N} \right) \end{aligned} \quad (7)$$

where the sum is over all binary words $\underline{a} = [a_1, \dots, a_N]$ of length N . Note that the second sub index specifies the space in which that part of the operator is acting. The expectation value for a measurement of the form in Eq. (4) is then

$$\begin{aligned} \langle \hat{M}_0 \rangle &= \text{Tr}(\hat{\rho} \hat{M}_0) \\ &= \sum_{\underline{a}} \bigotimes_{j=1}^N \text{Tr}(G_{1(j)}^{a_1} G_{2(j)}^{a_2} \dots G_{N(j)}^{a_N} \hat{m}) \end{aligned} \quad (8)$$

For graph states, the $G_{i(j)}$ correspond to a mapping of the adjacency matrix A , according to $G_{j(j)} = \sigma_x$, $G_{i(j)} = \sigma_I$ if $A_{ij} = 0$ and $G_{i(j)} = \sigma_z$ if $A_{ij} = 1$. Consequently

a term from the product in Eq. (8) contains either one factor of σ_x (if $a_j = 1$) or none (if $a_j = 0$) together with a number of factors of σ_z equal to the edge count v_j of node j ; it may be written in the canonical form $\sigma_x \sigma_z^{v_j}$ by swapping σ_x with those σ_z terms on its left. In doing so, each swap introduces a change of sign as $\sigma_x \sigma_z + \sigma_z \sigma_x = 0$ and the final results may be reduced depending on whether the edge count v_j is even (when $\sigma_x \sigma_z^{v_j} = \sigma_x$) or odd (when $\sigma_x \sigma_z^{v_j} = \sigma_x \sigma_z = -i\sigma_y$). As a result each trace in Eq. (8) evaluates to

$$\begin{aligned} & \text{Tr}(G_{1j}^{a_1} \dots G_{nj}^{a_n} \hat{m}) \\ &= (-1)^{\frac{1}{2}(a_j(A\mathbf{a}^T)_j + a_j r_j)} \begin{cases} \text{Tr}(\hat{m}) & (a_j, r_j) = (0, 0) \\ \text{Tr}(\hat{\sigma}_x \hat{m}) & (a_j, r_j) = (1, 0) \\ \text{Tr}(\hat{\sigma}_y \hat{m}) & (a_j, r_j) = (1, 1) \\ \text{Tr}(\hat{\sigma}_z \hat{m}) & (a_j, r_j) = (0, 1) \end{cases} \end{aligned} \quad (9)$$

Here the prefactor in Eq. (9) keeps track of the number of swaps and r_j is the parity of the edge count v_j , i.e. $r_j = 1$ if $(A\mathbf{a}^T)_j$ is odd and is 0 otherwise.

What then remains is to choose measurements \hat{m}, \hat{m}_0 and \hat{m}_1 as to provide a means of distinguishing non-isomorphic graphs. We consider a possibility for each case in the following sections. In section IIIB below measurements from the equal-angle slice of the Wigner function are used which have the form in Eq. (4) and treat no qubits differently. This results in a natural graph invariant which identifies more than 99.8% of the graphs we have tested, outperforming all of the classical invariants we consider. In section IIIC following the next one we consider a measurement distinguishing one qubit is distinguished as in Eq. (5). The resulting invariant can identify all graphs we have tested when combined with the eigenvalues of the adjacency matrix. Finally, in section IIID, we extend this scheme to the measurement of two qubits with an operator other than \hat{m}_0 , giving an invariant which has, on its own, distinguished all graphs we have tested.

B. Measurements which distinguish no qubits: the equal-angle slice of the Wigner function

To perform identical measurements on all qubits we used the equal-angle slice of the Wigner function which has previously been used for state characterization [34]. This lead us to speculate that it could be used to identify graph states. The results in Fig. 2 where we show the equal-angle slice of the Wigner function for all 34 non-isomorphic 5-node graphs supported this speculation [38]. We show in Fig. 3 example experimental data calculated on the IBM quantum experience. We note that we have made use of the Wigner function methods that have recently been included in the The Quantum Information Software Kit (QISKit) that “*is a software development kit (SDK) for working with OpenQASM and the IBM Q experience (QX)*” [39].

A detailed discussion of spin Wigner functions goes beyond the scope of this paper - please see Refs [33, 34, 40] for a full discussion. In brief, a spin Wigner function for a set of N qubits may be given in the form

$$W(\boldsymbol{\theta}, \boldsymbol{\phi}) = \langle \hat{\Pi}(\boldsymbol{\theta}, \boldsymbol{\phi}) \rangle = \text{Tr} \left[\hat{\Pi}(\boldsymbol{\theta}, \boldsymbol{\phi}) \hat{\rho} \right]. \quad (10)$$

Here $\boldsymbol{\theta} = (\theta_1, \dots, \theta_N)$ and $\boldsymbol{\phi} = (\phi_1, \dots, \phi_N)$ are the sets of Euler angles, as used in the Bloch sphere, associated with each qubit, and $\hat{\Pi}(\boldsymbol{\theta}, \boldsymbol{\phi})$ is a rotated generalised parity operator given by

$$\hat{\Pi}(\boldsymbol{\theta}, \boldsymbol{\phi}) = \bigotimes_{i=1}^N \hat{\Pi}_{\frac{1}{2}}^{(i)}(\theta_i, \phi_i). \quad (11)$$

All the $\hat{\Pi}_{\frac{1}{2}}^{(i)}$ have the same form and are given by [34]

$$\hat{\Pi}_{\frac{1}{2}}^{(i)} = \frac{1}{2} \begin{pmatrix} 1 + \sqrt{3} \cos \theta_i & -\sqrt{3} \sin \theta_i \exp(i\phi_i) \\ -\sqrt{3} \sin \theta_i \exp(-i\phi_i) & 1 - \sqrt{3} \cos \theta_i \end{pmatrix}. \quad (12)$$

The equal-angle slice, required for treating all qubits equivalently, is then obtained by setting $\theta_i = \theta$ and $\phi_i = \phi$ for all i . This gives an operator in a form equivalent to that in Eq. (4). Inserting $\hat{\Pi}(\boldsymbol{\theta}, \boldsymbol{\phi})$ into Eq. (8) gives the equal-angle slice of the Wigner Function as;

$$\begin{aligned} W(\theta, \phi) &= \sum_{\mathbf{a}} (-1)^{\frac{1}{2}(aA\mathbf{a}^T + a \cdot r)} \text{Tr}(\hat{\sigma}_y \hat{\Pi}_{\frac{1}{2}})^{a \cdot r} \times \\ & \text{Tr}(\hat{\sigma}_x \hat{\Pi}_{\frac{1}{2}})^{(1-r) \cdot a} \text{Tr}(\hat{\sigma}_z \hat{\Pi}_{\frac{1}{2}})^{(1-a) \cdot r} \end{aligned} \quad (13)$$

Evaluating the trace terms as

$$\begin{aligned} \text{Tr}(\hat{\Pi}_{\frac{1}{2}}) &= 1 \\ \text{Tr}(\hat{\sigma}_x \hat{\Pi}_{\frac{1}{2}}) &= -\sqrt{3} \sin \theta \cos \phi \\ \text{Tr}(\hat{\sigma}_y \hat{\Pi}_{\frac{1}{2}}) &= \sqrt{3} \sin \theta \sin \phi \\ \text{Tr}(\hat{\sigma}_z \hat{\Pi}_{\frac{1}{2}}) &= \sqrt{3} \cos \theta \end{aligned} \quad (14)$$

leads to the final expression

$$\begin{aligned} W(\theta, \phi) &= \sum_{\mathbf{a}} (-1)^{\frac{1}{2}(aA\mathbf{a}^T - a \cdot r) + 1 \cdot a} \sqrt{3}^{1 \cdot (a+r) + a \cdot r} \\ & \times \cos^{(1-a) \cdot r} \theta \sin^{1-a} \theta \cos^{(1-r) \cdot a} \phi \sin^{a \cdot r} \phi \quad (15) \\ &= \sum_{\mathbf{a}} C_{\mathbf{a}, r} x^{(1-r) \cdot a} y^{a \cdot r} z^{(1-a) \cdot r} \end{aligned}$$

where the second expression comes from using the notation $x = \sin \theta \cos \phi$, $y = \sin \theta \sin \phi$, $z = \cos \theta$ and

$$C_{\mathbf{a}, r} = (-1)^{\frac{1}{2}(aA\mathbf{a}^T - a \cdot r) + 1 \cdot a} \sqrt{3}^{1 \cdot (a+r) - a \cdot r}. \quad (16)$$

It is interesting to note that by analyzing coefficients of the terms in the polynomial it is possible to determine a number of permutation invariant properties of the adjacency matrix, such as the degree sequence. This supports

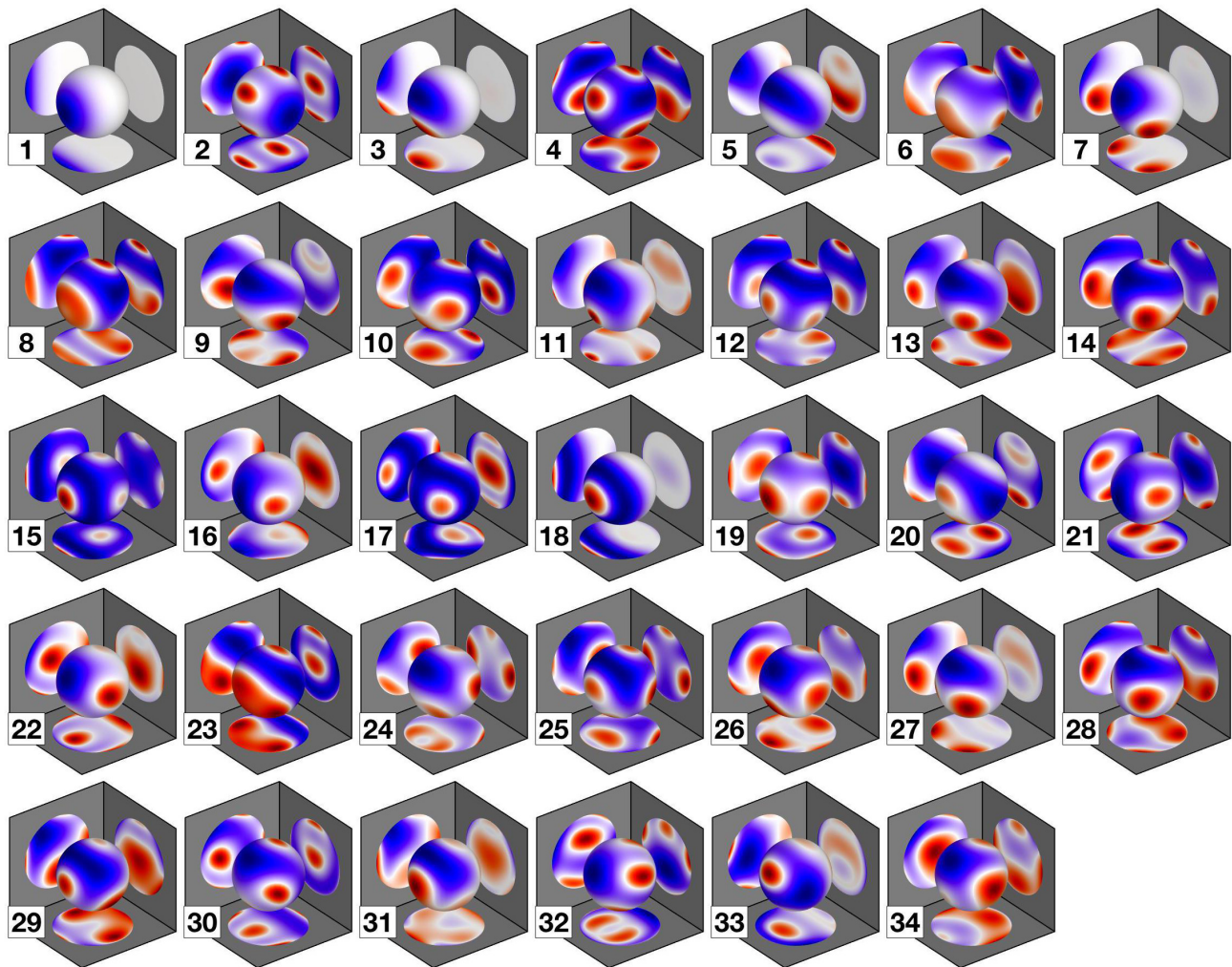


FIG. 2. We show the Wigner functions for the set of all five-node graphs that are not isomorphic. Note that the colour maps have been scaled for each figure to maximise the feature clarity. We have done this to better enable the reader to see the functional form of each graph (this does however mean that a direct comparison between plots in terms of magnitude is not possible). We have also computed the Wigner functions for all graphs of less than ten nodes and can use them to identify all graphs of less than eight nodes. Graphs with eight or nine nodes can still be efficiently identified by using anagraph measurements which have the form given in Eq. (18).

the possibility that equal-angle Wigner functions could fully encode the adjacency matrix (up to permutations), and in turn be used to distinguish all graph states.

However, as shown in Table (I) we have found sets of non-isomorphic graphs which have the same equal-angle slice of the Wigner function. We call graphs with the same equal-angle slice *equiumbral* [41]. Thus isomorphic implies equiumbral but the converse does not hold. Despite this it is worth noting that the equal-angle slice of the Wigner function is dependent upon enough information in the states to identify more than 99.8% of the graphs we have tested, significantly outperforming all the classical methods we have considered as shown in Table (I).

More generally we have found that any observable of the form in Eq. (4) will not be able distinguish all graph states, despite their use in permutation invariant tomog-

raphy [42].

This is due to the existence of non-isomorphic graphs which share the same number of each type of Pauli operator within each group element. Since these graph states are not isomorphic they cannot be made equal by permutations of the whole group; which is equivalent to permuting nodes. However, they can be made identical by applying permutations to a subset of the group elements. Thus we find that ‘equal-angle’ or ‘permutation invariant’ measurements, are actually invariant for a larger class of possible ‘reorderings’ including the partial permutations described above, and do not form an exclusively permutation invariant measurement.

This problem is overcome in following sections with measurements which are sensitive to partial permutations of the group.

We now consider the efficiency with which this method

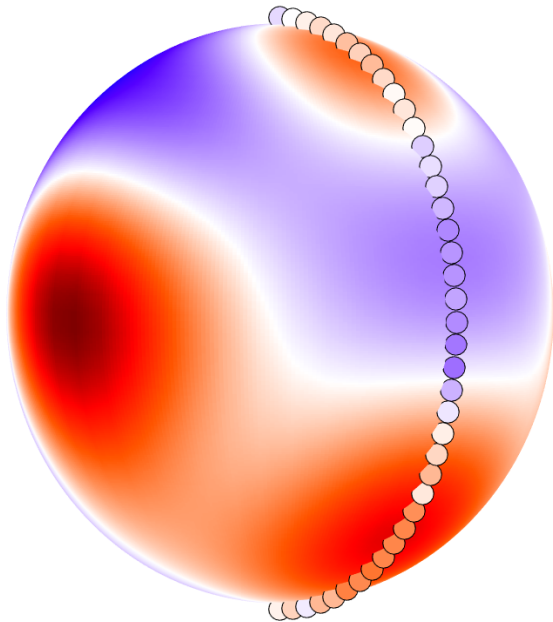


FIG. 3. Figure showing the equal-angle Wigner function for graph number 34 in Fig. 2. The sphere is the theoretical plot and the discs on its surface show the experimental data, calculated on the IBM quantum experience. We note that the IBM experience machines are still in development and that the deviations between theory and experiment seen here are to be expected. We also experienced some issues with the ϕ rotations on the hardware and therefore only show experimental data for $\phi_i = 0$. However, we were able to use the simulator in the IBM experience to obtain exact agreement with our own theoretical predictions, showing the process works in principle.

can be used to check if graphs are isomorphic. If ensemble measurements at P points are required to distinguish two non-isomorphic graphs, then using the $\mathcal{O}(N)$ construction of the state, the whole procedure will require $\mathcal{O}(PN)$ operations. Determining with certainty that two graphs are equiangular will require at most $P = N^2$ ensemble measurements per graph. Since non-isomorphic graphs may be distinguished in far fewer than N^2 ensemble measurements, the total procedure will require between $\mathcal{O}(N)$ and $\mathcal{O}(N^4)$ gate operations and ensemble measurements, dependent upon the graphs to be compared and the method of constructing the states. However, this analysis assumes negligible error in the ensemble measurements. Assuming a measurement process similar to that used in IBM's quantum computers, the number of preparations required per ensemble to distinguish pairs of graphs based on a single point appears to grow exponentially. As such, an equal-angle approach may require alternative measurement procedures to effectively obtain the functions with sufficient clarity. Whether alternative procedures are possible which are significantly more efficient at distinguishing these functions is left to further work. However, it may not be an issue as the method we

discuss in the next section should bypass such difficulties.

C. Measurements which distinguish a single qubit

Having established a class of measurements which depend upon the group elements in their entirety it is natural to try to determine information from the group elements which corresponds only to individual qubits. This can be done with an observable in the form of the second case, as given in Eq. (5), by taking

$$\hat{m}_0 = \hat{\sigma}_I + \hat{\sigma}_x + \hat{\sigma}_y + \hat{\sigma}_z \quad (17)$$

and taking \hat{m}_1 in turn to be $\hat{\sigma}_I$, $\hat{\sigma}_x$, $\hat{\sigma}_y$ and $\hat{\sigma}_z$, giving

$$\hat{M}_i^k = \bigotimes_{j=1}^N (\delta_{jk} \hat{\sigma}_i + (1 - \delta_{jk}) \hat{m}_0) \quad (18)$$

for qubit k and Pauli matrix i .

Substituting \hat{m}_0 for \hat{m} into Eq. (9), the trace terms for $j \neq k$ are all equal to 2, while the terms

$$[\text{Tr}(\hat{m}_1), \text{Tr}(\hat{\sigma}_x \hat{m}_1), \text{Tr}(\hat{\sigma}_y \hat{m}_1), \text{Tr}(\hat{\sigma}_z \hat{m}_1)] \quad (19)$$

will give $[2, 0, 0, 0]$, $[0, 2, 0, 0]$, $[0, 0, 2, 0]$ and $[0, 0, 0, 2]$, respectively for $\hat{m}_1 = \hat{\sigma}_I$, $\hat{\sigma}_x$, $\hat{\sigma}_y$ and $\hat{\sigma}_z$. As a consequence, the factor of 2^N cancels the normalization of the graph state and measuring $\hat{m}_1 = \hat{\sigma}_I$, $\hat{\sigma}_x$, $\hat{\sigma}_y$ and $\hat{\sigma}_z$ on qubit k , and \hat{m}_0 on the rest will yield a matrix \mathcal{M} of integer values dependent upon the number of occurrences of the operator i in the k^{th} space of the group elements, given by;

$$\begin{bmatrix} M_I^k \\ M_x^k \\ M_y^k \\ M_z^k \end{bmatrix} = \sum_{\underline{a}} (-1)^{\frac{1}{2}(\underline{a} A \underline{a}^T - \underline{a} \cdot \underline{x}) + 1 \cdot \underline{a}} \begin{bmatrix} (1 - a_k)(1 - r_k) \\ a_k(1 - r_k) \\ a_k r_k \\ (1 - a_k)r_k \end{bmatrix}. \quad (20)$$

The resulting $4N$ integers, when sorted by column k , provides a matrix which is invariant under any permutation of the qubits.

As an example of how to perform such a measurement experimentally, consider 'counting' the number of $\hat{\sigma}_x$ operators on the second qubit. Thus our operator will have a $\hat{\sigma}_x$ in the space of the second qubit. In the space of all other qubits the operator $\hat{\sigma}_I + \hat{\sigma}_x + \hat{\sigma}_y + \hat{\sigma}_z$ is measured. This corresponds to measuring $\sqrt{3}\hat{U}(\theta, \phi)\hat{\sigma}_z\hat{U}^\dagger(\theta, \phi)$, with $\theta = -\arctan(\sqrt{2})$, $\phi = -\pi/4$ and $\hat{U}(\theta, \phi) = \exp(i\phi\hat{\sigma}_z/2)\exp(i\theta\hat{\sigma}_y/2)$ [44].

Unfortunately the sorted matrix \mathcal{M} with elements M_i^k can be the same for non isomorphic graphs. Two graphs with identical matrices \mathcal{M} we term *anagraphs*, since they appear to contain the same number of each Pauli operator in the space of each qubit. We therefore have that

TABLE I. Rows 1, 5, 6 and 7 show values derived from “The On-Line Encyclopedia of Integer Sequence” [43] giving, for each graph up to 9 nodes the number of; graphs (A000088), the completeness gap of degree sequences, i.e. the number of graphs minus the number of degree sequences (A004251), the number of graphs minus the number of graphs with a unique Tutte polynomial (A243049), and the completeness gap of eigenspectra (A099883). In each row we show the ‘completeness gap’ which is determined as the number of graphs minus the number of distinct outcomes for a given invariant. Thus it gives an idea of how far an invariant is from being complete, i.e. able to distinguish all graphs. Rows 2, 3 and 4 show the completeness gaps using our quantum methods alone. Notably, in row 2 we have found we can distinguish at least all graphs with less than 10 nodes by performing anagraph measurements on 2 qubits simultaneously. Finally rows 8, 9 and 10 show the completeness gaps when combining methods. As shown in row 9 we find that combining anagraph measurements with eigenspectra allows for all graphs of less than 10 nodes to be distinguished.

Row #	Number of Nodes	1	2	3	4	5	6	7	8	9
1	Number of graphs	1	2	4	11	34	156	1,044	12,346	274,668
2	Completeness gap of dianagraph values	0	0	0	0	0	0	0	0	0
3	Completeness gap of equal-angle Wigner functions	0	0	0	0	0	0	0	14	222
4	Completeness gap of anagraph values	0	0	0	0	0	0	0	18	1,174
5	Completeness gap of eigenspectra	0	0	0	0	1	4	38	661	242,620
6	Completeness gap of Tutte Polynomials	0	0	0	4	15	84	548	5,629	90,776
7	Completeness gap of degree sequences	0	0	0	0	3	54	702	11,133	270,307
8	Completeness gap of eigenspectra & equal-angle Wigner functions	0	0	0	0	0	0	0	0	18
9	Completeness gap of eigenspectra & anagraphs values	0	0	0	0	0	0	0	0	0
10	Completeness gap of anagraphs & equal-angle Wigner functions	0	0	0	0	0	0	0	2	3

graphs which are isomorphic will be anagraphs but not the converse.

Despite this we have found that graphs which are anagraphs and isospectral are isomorphic in all cases we have considered. It is not known whether this holds generally. However, in the next section we introduce a measurement which is robust against the failure modes of both the equal angle and single qubit approaches.

We now consider the efficiency with which anagraph measurements can be used to check if graphs are isomorphic. Since each operator of the four operators $\hat{\sigma}_1, \hat{\sigma}_x, \hat{\sigma}_y$ and $\hat{\sigma}_z$ must be measured on each qubit there are $4N$ ensemble measurements to perform. Using the $\mathcal{O}(N)$ construction of the state, the whole procedure will require $\mathcal{O}(4N^2)$ gate operations and ensemble measurements. Furthermore, since the expectation values are integers the determination of the values should require a smaller number of shots per ensemble measurement than with the equal-angle method. This method is thus much more efficient than the phase space method we discussed above.

Whether or not the measurement problems of equal-angle methods are avoidable with either algorithmic changes such as incorporating information from several points, or hardware changes; a quantum device is necessary to achieve the efficiencies mentioned. Importantly the only required operations are local rotations, CZ operators and measurements in the computational basis which are all available on conventional quantum systems.

D. Measurements distinguishing two or more qubits

A whole family of operators can be formed by varying the number of qubits which are measured with a different operator to \hat{m}_0 . The equal-angle slice is an example with no qubits being measured with a different operator (although we rotate \hat{m}_0 to obtain more information about the state). We then vary a single operator on individual qubits to give the anagraph values. Following a similar regime, but distinguishing two qubits at a time by measuring them with Pauli operators instead of \hat{m}_0 , we find that at least all graphs with less than 10 nodes can be distinguished as well as all strongly regular graphs shown in row 2 of Table (I) and Table (III). This gives a measurement operator of the form

$$\hat{M}_2 = \bigotimes_{j=1}^N (\delta_{jq} \hat{m}_1 + \delta_{jp} \hat{m}_2 + (1 - \delta_{jq})(1 - \delta_{jp}) \hat{m}_0), \quad (21)$$

provided $(q, \hat{m}_1) \neq (p, \hat{m}_2)$. \hat{m}_2 is chosen similarly to \hat{m}_1 as any of the Pauli matrices and \hat{m}_0 is as in Eq. (17). We call operators of this form dianagraph operators. To remain permutation invariant all possible pairs must be measured and in general for k distinguished qubits there will be ‘ N choose k ’ sets which must be measured. Furthermore, if all possible combinations of Pauli matrices (including $\hat{\sigma}_I$) are measured on each qubit in a chosen set of k qubits, the number of measurements required per set increases exponentially as 4^k .

Whether this family of operators is applicable to solving the graph isomorphism problem is unclear, however they show promise in that the forms with $k = 1$ and 2

TABLE II. The table below shows the number of 9-node graphs which share the same equal-angle Wigner function, anagraph values or eigenvalues. Note that all observed equiumbral graphs fail only in pairs, whilst anagraphs can share common values with more than one other graph. All 8-node graphs which fail, only fail pairwise for all methods.

Degeneracy(set size)	2	3	4	5	6	7	8	9	10
Equiumbral sets	222	0	0	0	0	0	0	0	0
Anagraph sets	345	13	0	0	1	0	1	0	0
Isospectral sets	25762	2015	551	95	37	1	2	0	2

TABLE III. The table below shows the classes of strongly regular graphs which have been distinguished using our invariants. The graphs were obtained from Spence’s [45] online catalogue. The parameters correspond to the number of nodes, the degree of the nodes, the number of common neighbours adjacent nodes have and finally the number of neighbours non-adjacent nodes have in common [46]. By definition graphs which permit these parameters are strongly regular.

SR Graph Parameters
16-6-2-2
25-12-5-6
26-10-3-4
28-12-6-4
29-14-6-7

have successfully distinguished all graphs we have been able to test. Based on this we conjecture that any pair of graphs with N nodes will be distinguishable using measurements from the $N + 1$ members of this family.

IV. RESULTS

Direct classical simulation of these methods scales exponentially. Despite this we have found it tractable to numerically evaluate all 288,266 graphs of less than ten nodes as well as all pairs of strongly regular graphs of up to 29 nodes. In each case finding both the equal-angle slice of the Wigner function and evaluating the anagraph values.

A summary of our results is given in Table (I), where our methods may be compared against classical graph invariants such as the number of isospectral graphs and Tutte polynomials. To determine the number of unique measurement results a hashmap was formed for each invariant. This involves mapping the results for each graph into a value known as a key. If two graphs have the same result they will have the same key but not otherwise. Associated with each key is the number of any graphs which have that key, where the graph’s number is determined by Maple 2017.3’s non-isomorphic graph generator. This method allows graphs with identical measurement results to quickly be found, as they will share the same key, whilst also allowing graphs with similar results

TABLE IV. This table shows the anagraph values of simple graph and a structurally similar instance of a fuzzy graph with noise applied to the edge weights. Each pair of rows shows the corresponding anagraph values from each graph type. The operator measured for that row is shown in brackets. The columns represent distinct qubits on which the operator was measured. The order is determined by sorting the anagraph values.

$(\hat{\sigma}_I)$ Simple Graph	6	6	6	6	8
Random Weighted Graph	6.60	6.52	6.53	6.68	8.71
$(\hat{\sigma}_x)$ Simple Graph	2	2	6	6	4
Random Weighted Graph	2.63	2.52	6.53	6.68	4.02
$(\hat{\sigma}_y)$ Simple Graph	6	6	2	2	0
Random Weighted Graph	6.77	6.87	2.75	2.94	0.67
$(\hat{\sigma}_z)$ Simple Graph	6	6	6	6	8
Random Weighted Graph	6.10	6.19	6.30	5.80	8.69

to be found and compared by sorting the hashmap by the keys and then comparing adjacent entries.

The number of graphs which share any particular key is smaller for the quantum invariants than the classical invariants. The degeneracy of these measures for nine node graphs is shown in Table (II). For the special case of non-isomorphic strongly regular graphs which scale badly for classical algorithms such as Nauty, we show the classes we have successfully distinguished in Table (III). We note that our invariants were also able to distinguish the pair of 24 node Mermin magic square graphs which were indistinguishable to the quantum approach of Asterias [47].

A. Extensions to weighted graphs

It should also be possible to apply our invariants to weighted graphs states, formed by the application of controlled phase gates as opposed to CZ gates. Equal-angle functions are order invariant for all states and as shown in Fig. 4, small variations in the edge weights appear to correspond to small variations in the equal-angle Wigner functions. We have also performed preliminary checks on anagraph measurements finding that graphs with a small phase difference have similar anagraph values. This is shown in Table (IV) where the anagraph values of a simple and similar instance of a fuzzy graph are given. A full investigation is left to future work.

V. CONCLUSION AND REMARKS

In this work we have introduced a family of new graph invariants which can be determined on a quantum simulator/computer. We have also shown that these invariants can distinguish a greater proportion of non-isomorphic graphs than classical invariants. Our strategy makes use of the fact that a quantum state uniquely representing

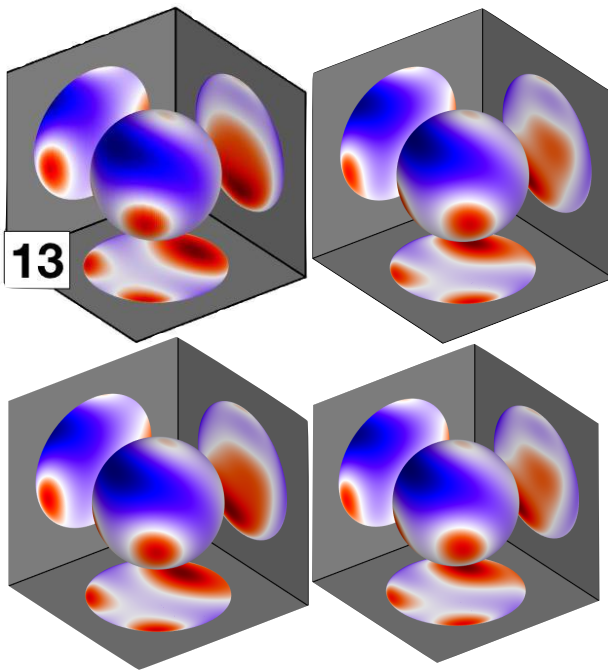


FIG. 4. Shown above in the first row are the equal-angle Wigner functions of the 5-node graph numbered 13 in Fig. 2 and a weighted graph which is structurally similar to it. In the second row we show fuzzy graphs also with a similar form. Due to weighted connections the resultant function is slightly distorted from that originally obtained on the left. However, the topography of the function appears to be robust to small changes in the edge weights.

a N node graph can be efficiently constructed using N^2 simple gate operations applied to an initial spin-coherent state on N qubits. This renders all the information about the graph into a state which may then be arbitrarily probed for relevant information. It is our belief that this will provide many opportunities for the discovery or creation of novel and powerful graph invariants, providing a promising step in understanding the graph isomorphism problem.

We have demonstrated the viability of such an approach by applying our method on the IBM Q experience. However, the overhead of setting up the quantum state and taking ensemble measurements means that, even in

the presence of a perfect implementation of a quantum computer, small graphs would be more efficiently checked classically. We therefore note that, as with other quantum algorithms, for this method to be practically deployed great advances are needed in realising large scale quantum computers.

Although our algorithms and the Weisfeiler-Lehman algorithms both perform graph canonisation, we believe there are key differences which make our algorithms distinct from their approach. The ability to distinguish strongly regular graphs shows our algorithms are not equivalent to 2 dimensional Weisfeiler-Lehman algorithm. Our procedure is not based on iterative refinement, instead we canonically construct a unique graph state and measure invariant properties from it. Furthermore, given the exponential resources on a quantum computer which are exploited by the algorithms, we conjecture that we may be accessing properties not observed in classical Weisfeiler-Lehman algorithms. Distinguishing the 80 node Cai-Fürer-Immerman graphs [26] would prove our algorithms are unrelated to Weisfeiler-Lehman's. However, it is not possible to evaluate such large graphs with current technology.

ACKNOWLEDGMENTS

We acknowledge use of the IBM Q experience for this work. The views expressed are those of the authors and do not reflect the official policy or position of IBM or the IBM Q experience team. R.P.R. is funded by the EPSRC [grant number EP/N509516/1]. T.T. notes that this work was supported in part by JSPS KAKENHI (C) Grant Number JP17K05569. S.J.D. acknowledges support from the Australian Research Council Centre of Excellence in Engineered Quantum Systems EQUS (Project CE110001013). We would also like to thank J. Stark, D. Bacon, S. Serverine and G. M. Fratangelo for their help suggesting example graphs to test our invariants. MJE would like to thank W. J. Munro for feedback and advice. MJE would like to thank Roberto Desimone and the InnovateUK “*quantum algorithms for optimised planning and scheduling*” project for providing current context on the importance of the graph isomorphism problem to industry. Please send queries on computational representation, modelling and optimisation to VMD, all other enquiries to MJE.

[1] F. Harary, *Graph Theory* (Addison-Wesley Publishing Company, Inc, 1972).
 [2] R. Gould, *Graph Theory* (Benjamin/Cummings Publishing Company, Inc, 1988).
 [3] R. M. C. Roberts and C. J. Fourie, IEEE Transactions on Applied Superconductivity **25**, 1 (2015).
 [4] A. C. Berg, T. L. Berg, and J. Malik, in *Computer Vision and Pattern Recognition, 2005. CVPR 2005. IEEE*

Computer Society Conference on, Vol. 1 (IEEE, 2005) pp. 26–33.
 [5] M. T. McCann, J. A. Ozolek, C. A. Castro, B. Parvin, and J. Kovacevic, IEEE Signal Processing Magazine **32**, 78 (2015).
 [6] C. Kruegel, E. Kirida, D. Mutz, W. Robertson, and G. Vigna, in *Recent Advances in Intrusion Detection*, edited by A. Valdes and D. Zamboni (Springer Berlin

- Heidelberg, Berlin, Heidelberg, 2006) pp. 207–226.
- [7] (2018), as was discussed in the QCAPS Innovation Workshop (4th July) at the BT Centre in London funded under the UK Quantum Technology Programme by InnovateUK.
- [8] M. Blum, ICM Proceedings: 1444–1451 (1986).
- [9] J. R. Ullmann, *J. ACM* **23**, 31 (1976).
- [10] B. D. McKay and A. Piperno, *Journal of Symbolic Computation* **60**, 94 (2014).
- [11] L. P. Cordella, P. Foggia, C. Sansone, and M. Vento, *IEEE Transactions on Pattern Analysis and Machine Intelligence* **26**, 1367 (2004).
- [12] L. Lovász, *Large networks and graph limits*, Vol. 60 (American Mathematical Society Providence, 2012).
- [13] B. Weisfeiler and A. Lehman, *Nauchno-Tekhnicheskaya Informatsiya (in Russian)*, 12 (1968).
- [14] G. Ryabov, https://www.itl.zcu.cz/wl2018/pdf/wl_paper_translation.pdf (2018), translation of ‘A Reduction of a Graph to a Canonical Form and an Algebra Arising during this Reduction’, Weisfeiler, (1968).
- [15] B. Weisfeiler, *On Construction and Identification of Graphs* (Springer, 1976).
- [16] L. Babai, “Graph isomorphism in quasipolynomial time,” (2015), arXiv:1512.03547.
- [17] H. A. Helfgott, J. Bajpai, and D. Dona, “Graph isomorphisms in quasi-polynomial time,” (2017), arXiv:1710.04574.
- [18] J. Y. Cai, M. Fürer, and N. Immerman, *Combinatorica* **12**, 389 (1992).
- [19] B. L. Douglas, “The Weisfeiler-Lehman Method and Graph Isomorphism Testing,” (2011), arXiv:1101.5211.
- [20] S. Arora and B. Barak, *Computational Complexity* (Cambridge University Press, New York, 2009).
- [21] P. W. Shor, *SIAM J. Comput.* **26**, 1484 (1997).
- [22] F. Gaitan and L. Clark, *Phys. Rev. A* **89**, 022342 (2014).
- [23] D. Aharonov, W. van Dam, J. Kempe, Z. Landau, S. Lloyd, and O. Regev, in *45th Annual IEEE Symposium on Foundations of Computer Science* (2004) pp. 42–51.
- [24] B. L. Douglas and J. B. Wang, *Journal of Physics A: Mathematical and Theoretical* **41**, 075303 (2008).
- [25] S. D. Berry and J. B. Wang, *Phys. Rev. A* **83**, 042317 (2011).
- [26] M. Fürer, “A Counterexample In Graph Isomorphism Testing,” <http://funkybee.narod.ru/misc/graphiso.pdf> (1987).
- [27] J. Smith, ArXiv e-prints (2010), arXiv:1004.0206 [quant-ph].
- [28] L. Zhao, C. A. Pérez-Delgado, and J. F. Fitzsimons, *Physical Review A* **93**, 032314 (2016), arXiv:1510.03742.
- [29] M. Hein, W. Dür, J. Eisert, R. Raussendorf, M. Van den Nest, and H. . Briegel, eprint arXiv:quant-ph/0602096 (2006), quant-ph/0602096.
- [30] M. Mhalla and S. Perdrix, arXiv preprint quant-ph/0412071, 17 (2004), arXiv:0412071 [quant-ph].
- [31] P. Høyer, M. Mhalla, and S. Perdrix, in *Algorithms and Computation*, edited by T. Asano (Springer Berlin Heidelberg, Berlin, Heidelberg, 2006) pp. 638–649.
- [32] A. Cabello, L. E. Danielsen, A. J. López-Tarrida, and J. R. Portillo, *Physical Review A - Atomic, Molecular, and Optical Physics* **83**, 1 (2011), arXiv:1011.5464.
- [33] T. Tilma, M. J. Everitt, J. H. Samson, W. J. Munro, and K. Nemoto, *Phys. Rev. Lett.* **117**, 180401 (2016).
- [34] R. P. Rundle, P. W. Mills, T. Tilma, J. H. Samson, and M. J. Everitt, *Phys. Rev. A* **96**, 022117 (2017).
- [35] E. P. Wigner, *Phys. Rev.* **40**, 749 (1932).
- [36] A. Rocchetto, “Stabiliser states are efficiently PAC-learnable,” (2017), arXiv:1705.00345.
- [37] M. A. Nielsen and I. L. Chuang, *Quantum Computation and Quantum Information: 10th Anniversary Edition*, 10th ed. (Cambridge University Press, New York, NY, USA, 2011).
- [38] We note for completeness that we have verified for a selection of graphs that their isomorphisms do indeed produce equiumbral plots.
- [39] IBM, “Qiskit - quantum information software kit,” (2018).
- [40] R. P. Rundle, T. Tilma, J. H. Samson, V. M. Dwyer, R. F. Bishop, and M. J. Everitt, “A general approach to quantum mechanics as a statistical theory,” (2018), arXiv:arXiv:1708.03814.
- [41] Meaning of equal shadow.
- [42] G. Tóth, W. Wieczorek, D. Gross, R. Krischek, C. Schwemmer, and H. Weinfurter, *Phys. Rev. Lett.* **105**, 250403 (2010).
- [43] N. Sloane, “The on-line encyclopedia of integer sequences (oeis),” <http://oeis.org> (2018).
- [44] We note that it is possible to adjust the above arguments to efficiently obtain from the graph-state density matrix the generators and therefore the adjacency matrix from a given graph state. This will be covered in a future paper, see also [48] for identifying stabilizer states.
- [45] T. Spence, <http://www.maths.gla.ac.uk/~es/index.php> (2018).
- [46] C. Godsil and G. Royle, *Algebraic Graph Theory* (Springer, New York, 2001).
- [47] A. Atserias, L. Mančinska, D. E. Roberson, R. Šámal, S. Severini, and A. Varvitsiotis, “Quantum and non-signalling graph isomorphisms,” (2016), arXiv:1611.09837.
- [48] A. Montanaro, “Learning stabilizer states by bell sampling,” (2017), arXiv:1707.04012.